Supplementary Information for "Model-data synthesis of benthic isotopes suggests a warmer Miocene Climatic Optimum"

Feng Zhu[1,*], Jiang Zhu[1], Weimin Si[2], Jared E. Nirenberg[2], Timothy Herbert[2], Jessica E. Tierney[3], R. Paul Acosta[4], Natalie J. Burls[4], and David Evans[5]

[1]Climate and Global Dynamics Laboratory, NSF National Center for Atmospheric Research, Boulder, CO, USA
[2]Department of Earth, Environmental and Planetary Sciences, Brown University, Providence, RI, USA
[3]Department of Geosciences, University of Arizona, Tucson, AZ, USA
[4]Department of Atmospheric, Oceanic and Earth Sciences, Center for Ocean-Land-Atmosphere Studies, George Mason University, Fairfax, VA, USA
[5]School of Ocean and Earth Science, University of Southampton, Southampton, UK
[*]Corresponding author: fengzhu@ucar.edu

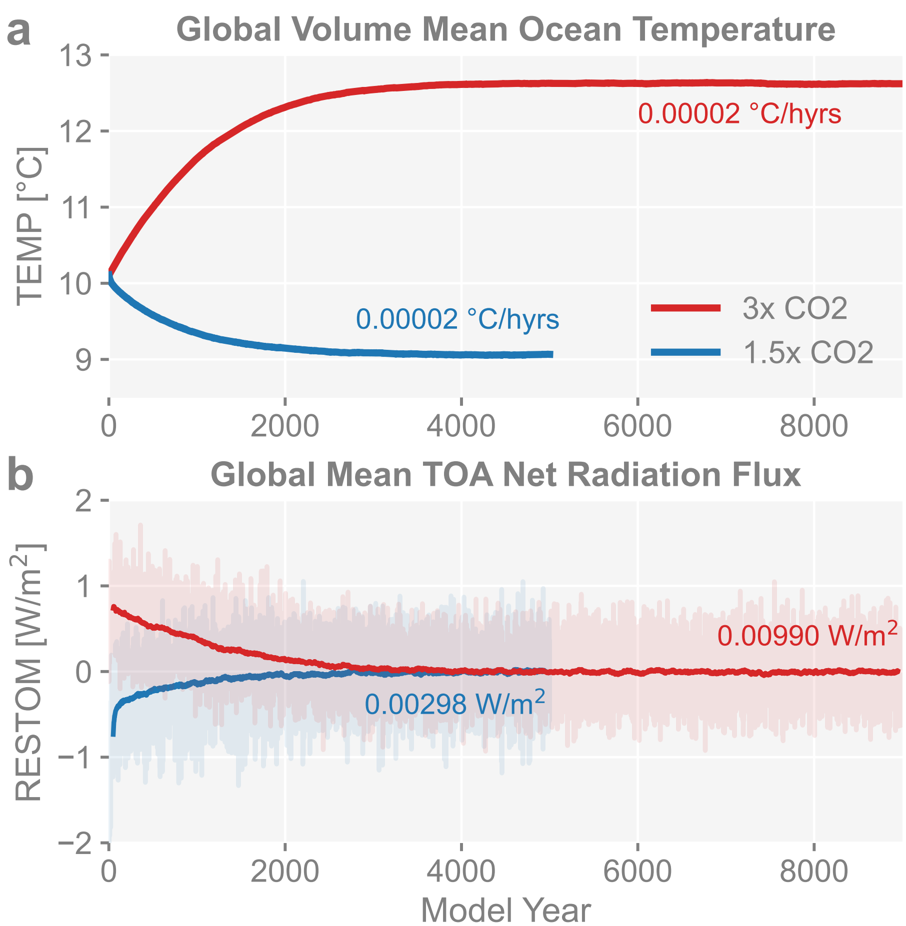

SI Fig. 1. The equilibrium in the long-run 1.5xCO2 and 3xCO2 simulations. **a** The global volume mean ocean temperature. **b** The global mean top-of-atmosphere (TOA) net radiation flux. The transparent curves indicate the annual mean, while the solid curves indicate the 100-year mean.

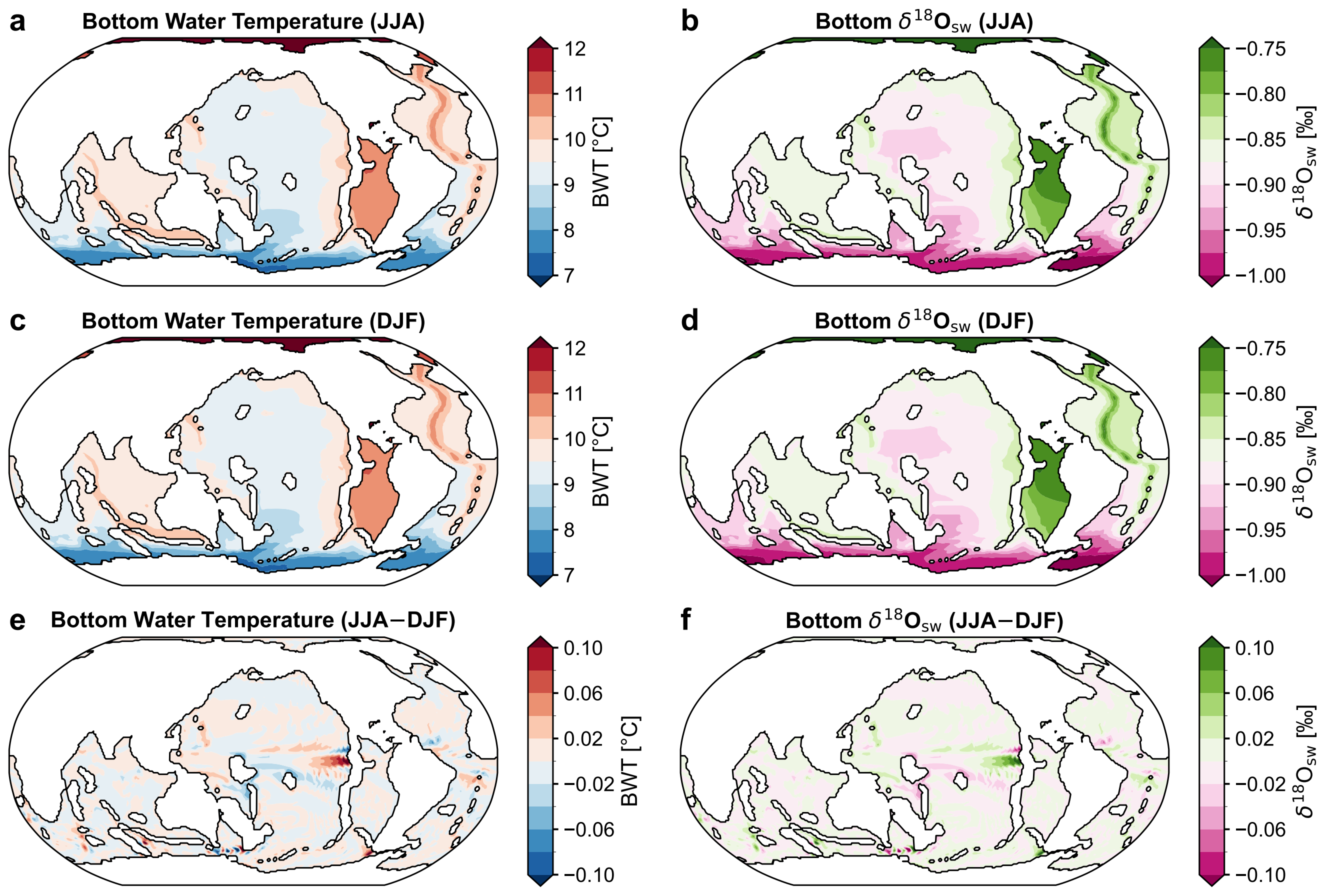

SI Fig. 2. The seasonal bottom (below 3 km) mean water temperature (BWT) and $\delta^{18}O_{sw}$ fields in the 3xCO2 simulation. a-b The boreal summer (JJA). **c-d** The boreal winter (DJF). **e-f** The small difference between the boreal summer and the boreal winter showing minimal seasonal variability.

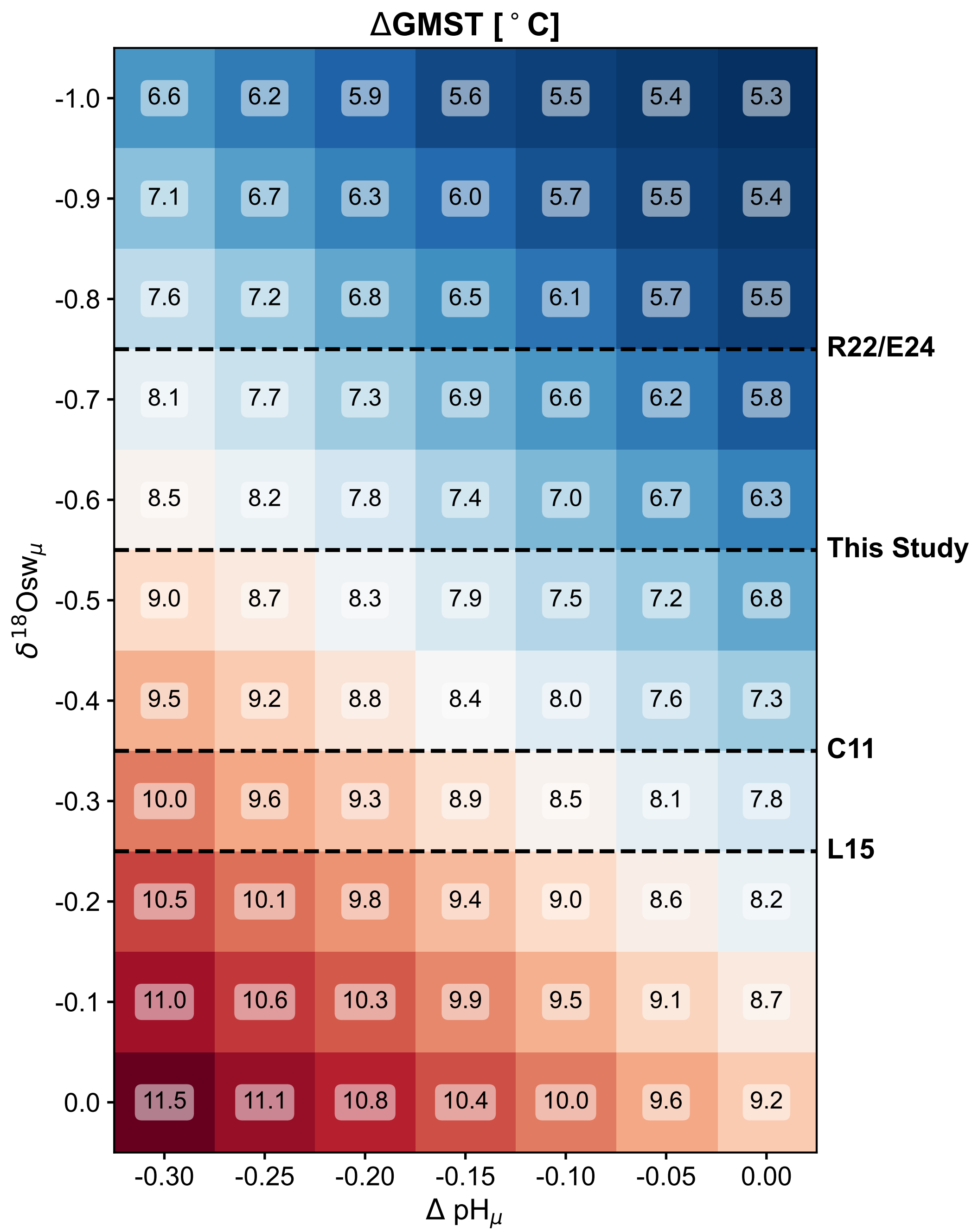

SI Fig. 3. The maximum likelihood (MLE) estimation of the Miocene Climatic Optimum (MCO) warmth in global mean surface temperature (GMST) relative to the preindustrial (PI) under different assumptions of the MCO global mean seawater pH and $\delta^{18}O_{sw}$. Different choices of the MCO global mean seawater $\delta^{18}O_{sw}$ are noted in the figure, including the one used in this study and those used in previous studys. R22/E24: Rohling et al. (2022)[2] and Evans et al. (2024)[3]; C11: Cramer et al. (2011)[4]; L15: Lear et al. (2015)[5].

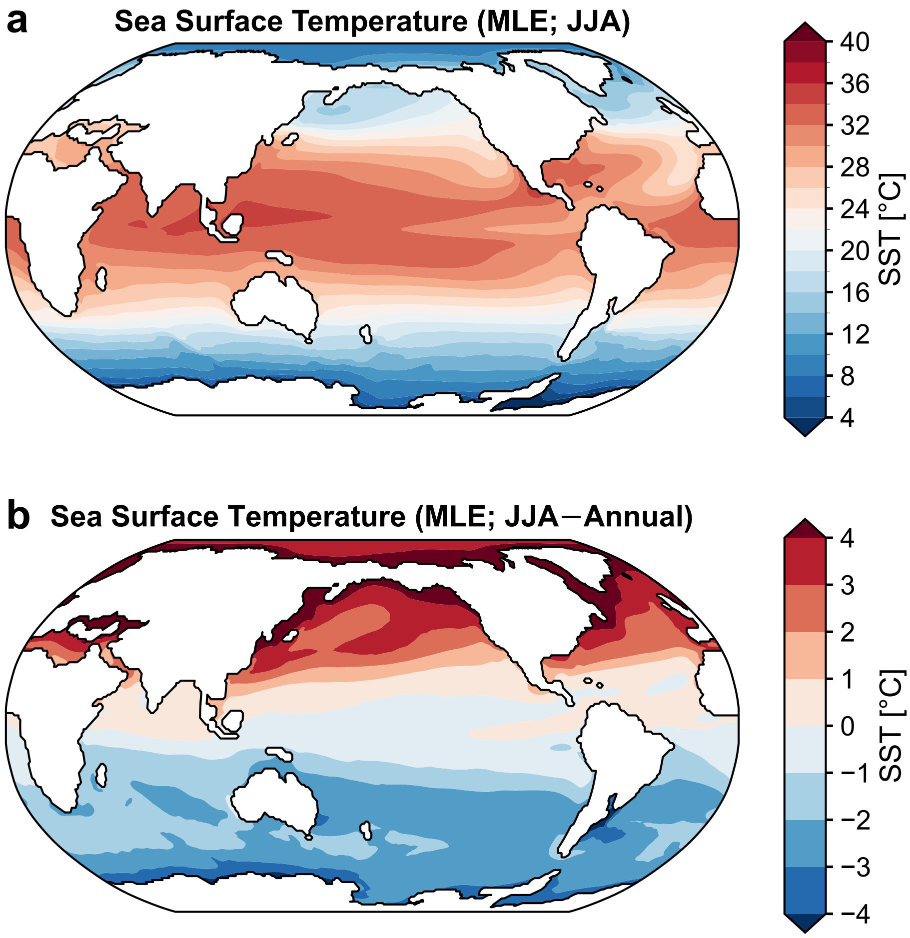

SI Fig. 4. The maximum likelihood estimation (MLE) of the boreal summer sea surface temperature (SST) field. a The boreal summer (JJA) field. **b** The difference between JJA and the annual mean (Annual).

Site ID	Paleo Lat (°)	Paleo Long (°)	Modern Lat (°)	Modern Long (°)	Depth (m)	Mean (‰)	SD (‰)
DSDP237[6]	-8.86	54.32	-7.08	58.12	1623	1.615500	0.170154
DSDP289[6]	-2.80	162.86	-0.50	154.91	2224	1.374615	0.209030
DSDP317[7]	-14.29	204.97	-11.00	197.74	2598	1.571786	0.220656
DSDP408[8]	61.03	334.06	63.38	330.99	1624	0.733333	0.041633
DSDP563[6,9]	31.73	317.92	33.64	316.00	3786	1.406970	0.242313
DSDP574[6,10]	1.14	228.98	8.00	226.67	4561	1.339695	0.217692
DSDP588[11]	-32.35	158.87	-26.11	159.93	1533	1.272273	0.313064
DSDP590[11]	-37.19	159.98	-31.17	159.96	1533	1.023529	0.253228
DSDP591[11]	-37.49	158.00	-31.58	158.95	2131	1.268750	0.342907
DSDP608[9]	40.96	328.92	42.84	325.96	3526	1.125833	0.206638
DSDP667[6]	2.66	334.69	4.57	336.99	3529	1.450750	0.247825
NGHP-01-01A[12]	10.45	64.55	15.30	70.90	2663	1.530889	0.595047
ODP704[9]	-49.37	3.30	-46.88	7.42	2541	1.055000	0.176777
ODP744[13]	-61.18	79.13	-61.57	79.90	2317	1.847778	0.234456
ODP747[9]	-54.49	74.96	-54.81	72.99	1695	1.586892	0.546643
ODP761[14]	-24.64	109.92	-16.74	115.54	2179	1.314253	0.153499
ODP806[15]	-2.02	162.95	0.32	154.96	2519	1.273939	0.262392
ODP1146[16]	20.86	113.00	19.46	117.01	2091	1.049022	0.290060
ODP1171[17]	-55.59	148.69	-48.50	151.00	2150	1.336810	0.208507
ODP1237[18]	-18.46	269.86	-16.01	283.62	3212	1.432607	0.248239
U1336[19]	4.76	235.00	7.70	231.75	4286	1.532886	0.197610
U1337[20]	1.03	232.00	3.83	236.79	4476	1.336185	0.270719
U1338[21]	-0.11	247.91	2.51	241.99	4210	1.448941	0.234350

SI Table 1. The benthic foraminiferal records during the Miocene Climatic Optimum (MCO) with paleo and modern locations. SD: standard deviation.

Site ID	Proxy	Paleo Lat (°)	Paleo Long (°)	Mean (°C)	SD (°C)
608[22]	UK37	41.33	336.48	28.7	1.5
608[22]	TEX86	41.35	336.49	28.9	4.4
730[23]	TEX86	7.30	57.19	32.7	2.1
761[24]	Mg/Ca	-23.74	112.50	29.2	2.0
884[25]	UK37	48.74	179.52	20.2	1.5
925[26]	UK37	2.55	321.59	28.1	1.5
925[26]	TEX86	2.55	321.59	28.1	2.5
926[27]	Mg/Ca	1.57	322.70	27.8	2.0
959[28,29]	TEX86	1.27	353.80	30.0	3.0
982[30]	UK37	56.56	342.53	27.5	1.5
982[31]	TEX86	56.03	342.66	25.4	3.0
982[31]	UK37	56.00	342.64	23.7	0.5
1171[17]	Mg/Ca	-55.57	149.76	16.6	2.0
1146[32]	Mg/Ca	21.29	117.66	27.8	2.0
U1338[33]	UK37	-7.50	254.10	28.7	1.5
U1356[34]	TEX86	-61.59	133.74	17.4	2.5
AND2A[35]	TEX86	-77.06	156.62	5.8	2.5

SI Table 2. The Miocene Climatic Optimum (MCO) sea surface temperature proxy records at various sites. SD: standard deviation.

References

1. Rohling, E. J. *et al.* Comparison and Synthesis of Sea-Level and Deep-Sea Temperature Variations Over the Past 40 Million Years. *Rev. Geophys.* **60**, e2022RG000775, DOI: 10.1029/2022RG000775 (2022).
2. Evans, D., Brugger, J., Inglis, G. N. & Valdes, P. The Temperature of the Deep Ocean Is a Robust Proxy for Global Mean Surface Temperature During the Cenozoic. *Paleoceanogr. Paleoclimatology* **39**, e2023PA004788, DOI: 10.1029/2023PA004788 (2024).
3. Cramer, B., Miller, K., Barrett, P. & Wright, J. Late cretaceousneogene trends in deep ocean temperature and continental ice volume: Reconciling records of benthic foraminiferal geochemistry (18o and mg/ca) with sea level history. *J. Geophys. Res. Ocean.* **116** (2011). Publisher: Wiley Online Library.
4. Lear, C. H. *et al.* Neogene ice volume and ocean temperatures: Insights from infaunal foraminiferal mg/ca paleothermometry. *Paleoceanography* **30**, 1437–1454 (2015). Number: 11 Publisher: Wiley Online Library.
5. Woodruff, F. & Savin, S. Mid-Miocene isotope stratigraphy in the deep sea: High-resolution correlations, paleoclimatic cycles, and sediment preservation. *Paleoceanography* **6**, 755–806, DOI: 10.1029/91PA02561 (1991).
6. Woodruff, F. & Savin, S. M. Miocene deepwater oceanography. *Paleoceanography* **4**, 87–140, DOI: 10.1029/PA004i001p00087 (1989).
7. Keigwin, L. D., Aubry, M.-P. & Kent, D. V. (Appendix) Stabile isotopes δ^1?O and δ^{13}C for DSDP Sites 37-334, 49-408, and 49-410 and Holes 81-552A, 94-610E, and 94-611C. DOI: 10.1594/PANGAEA.788680 (PANGAEA, 1987). In supplement to: Keigwin, LD et al. (1987): North Atlantic late Miocene stable-isotope stratigraphy, biostratigraphy, and magnetostratigraphy. In: Ruddiman, WF; Kidd, RB; Thomas, E; et al. (eds.), Initial Reports of the Deep Sea Drilling Project, Washington (U.S. Govt. Printing Office), 94, 935-963, https://doi.org/10.2973/dsdp.proc.94.130.1987.
8. Wright, J. D., Miller, K. G. & Fairbanks, R. G. Early and Middle Miocene stable isotopes: Implications for Deepwater circulation and climate. *Paleoceanography* **7**, 357–389, DOI: 10.1029/92PA00760 (1992).
9. Pisias, N. G., Shackleton, N. J. & Hall, M. A. (Table 1) Stable isotope ratios of benthic foraminifera from DSDP Hole 85-574A. DOI: 10.1594/PANGAEA.803485 (PANGAEA, 1985). In supplement to: Pisias, NG et al. (1985): Stable isotope and calcium carbonate records from hydraulic piston cored Hole 574A: high-resolution records from the middle Miocene. In: Mayer, L; Theyer, E; et al. (eds.), Initial Reports of the Deep Sea Drilling Project, Washington (U.S. Govt. Printing Office), 85, 735-748, https://doi.org/10.2973/dsdp.proc.85.121.1985.
10. Kennett, J. P. (Appendix A1) Oxygen and carbon isotope composition of benthic foraminifera from DSDP Site 90-588. DOI: 10.1594/PANGAEA.729767 (PANGAEA, 1986). In supplement to: Kennett, JP (1986): Miocene to early Pliocene oxygen and carbon isotope stratigraphy in the Southwest Pacific, Deep Sea Drilling Project Leg 90. In: Kennett, JP; von der Borch, CC; et al. (eds.), Initial Reports of the Deep Sea Drilling Project, Washington (U.S. Govt. Printing Office), 90, 1383-1411, https://doi.org/10.2973/dsdp.proc.90.142.1986.
11. Steinke, S., Lin, G., Chen, A. & Groeneveld, J. Planktic foraminiferal stable isotopes, Mg/Ca, local seawater d18O and temperature differences of sediment core NGHP-01-01A, DOI: 10.1594/PANGAEA.961229 (2024).
12. Majewski, W. Mid-Miocene invasion of ecological niches by planktonic foraminifera of the Kerguelen Plateau, Antarctica. *Mar. Micropaleontol.* **46**, 59–81, DOI: 10.1016/S0377-8398(02)00051-8 (2002).
13. Lear, C. H., Mawbey, E. M. & Rosenthal, Y. Cenozoic benthic foraminiferal Mg/Ca and Li/Ca records: Toward unlocking temperatures and saturation states. *Paleoceanography* **25**, DOI: 10.1029/2009PA001880 (2010).
14. Corfield, R. M. & Cartlidge, J. E. (Appendix B) Stable carbon and oxygen isotope ratios of bulk rock samples and foraminifera of ODP Hole 130-806B. DOI: 10.1594/PANGAEA.780105 (PANGAEA, 1993). In supplement to: Corfield, RM; Cartlidge, JE (1993): Oxygen and carbon isotope stratigraphy of the Middle Miocene, Holes 805B and 806B. In: Berger, WH; Kroenke, LW; Mayer, LA; et al. (eds.), Proceedings of the Ocean Drilling Program, Scientific Results, College Station, TX (Ocean Drilling Program), 130, 307-322, https://doi.org/10.2973/odp.proc.sr.130.026.1993.
15. Holbourn, A. E. *et al.* Late Miocene climate cooling and intensification of southeast Asian winter monsoon. *Nat. Commun.* **9**, 1584, DOI: 10.1038/s41467-018-03950-1 (2018).
16. Shevenell, A. E., Kennett, J. P. & Lea, D. W. Middle Miocene Southern Ocean Cooling and Antarctic Cryosphere Expansion. *Science* **305**, 1766–1770, DOI: 10.1126/science.1100061 (2004).
17. Holbourn, A., Kuhnt, W., Schulz, M., Flores, J.-A. & Andersen, N. Orbitally-paced climate evolution during the middle Miocene "Monterey" carbon-isotope excursion. *Earth Planet. Sci. Lett.* **261**, 534–550, DOI: 10.1016/j.epsl.2007.07.026 (2007).

18. Voigt, J., Hathorne, E. C., Frank, M. & Holbourn, A. Minimal influence of recrystallization on middle Miocene benthic foraminiferal stable isotope stratigraphy in the eastern equatorial Pacific. *Paleoceanography* **31**, 98–114, DOI: 10.1002/2015PA002822 (2016).

19. Holbourn, A., Kuhnt, W., Kochhann, K. G., Andersen, N. & Sebastian Meier, K. Global perturbation of the carbon cycle at the onset of the Miocene Climatic Optimum. *Geology* **43**, 123–126, DOI: 10.1130/G36317.1 (2015).

20. Holbourn, A. *et al.* Middle Miocene climate cooling linked to intensification of eastern equatorial Pacific upwelling. *Geology* **42**, 19–22, DOI: 10.1130/G34890.1 (2014).

21. Super, J. R. *et al.* North Atlantic temperature and pCO2 coupling in the early-middle Miocene. *Geology* **46**, 519–522, DOI: 10.1130/G40228.1 (2018).

22. Zhuang, G., Pagani, M. & Zhang, Y. G. Monsoonal upwelling in the western Arabian Sea since the middle Miocene. *Geology* **45**, 655–658, DOI: 10.1130/G39013.1 (2017).

23. Sosdian, S. M., Babila, T. L., Greenop, R., Foster, G. L. & Lear, C. H. Ocean Carbon Storage across the middle Miocene: A new interpretation for the Monterey Event. *Nat. Commun.* **11**, 134, DOI: 10.1038/s41467-019-13792-0 (2020).

24. Nirenberg, J. E. & Herbert, T. D. North Pacific warmth synchronous with the Miocene Climatic Optimum. *Geology* DOI: 10.1130/G52432.1 (2024).

25. Zhang, Y. G., Pagani, M., Liu, Z., Bohaty, S. M. & DeConto, R. A 40-million-year history of atmospheric CO2. *Philos. Transactions Royal Soc. A: Math. Phys. Eng. Sci.* **371**, 20130096, DOI: 10.1098/rsta.2013.0096 (2013).

26. Sosdian, S. M. *et al.* Constraining the evolution of Neogene ocean carbonate chemistry using the boron isotope pH proxy. *Earth Planet. Sci. Lett.* **498**, 362–376, DOI: 10.1016/j.epsl.2018.06.017 (2018).

27. van der Weijst, C. M. H. *et al.* A 15-million-year surface- and subsurface-integrated TEX_{86} temperature record from the eastern equatorial Atlantic. *Clim. Past* **18**, 1947–1962, DOI: 10.5194/cp-18-1947-2022 (2022).

28. Wubben, E. *et al.* Tropical Warming and Intensification of the West African Monsoon During the Miocene Climatic Optimum. *Paleoceanogr. Paleoclimatology* **39**, e2023PA004767, DOI: 10.1029/2023PA004767 (2024).

29. Herbert, T. D. *et al.* Late Miocene global cooling and the rise of modern ecosystems. *Nat. Geosci.* **9**, 843–847, DOI: 10.1038/ngeo2813 (2016).

30. Super, J. R. Biomarker indicies proxies from different Holes of ODP Site 162-982, DOI: 10.1594/PANGAEA.913801 (2010).

31. Holbourn, A. E. Sea surface and subsurface temperature reconstruction for ODP Site 184-1146, DOI: 10.1594/PANGAEA.861237 (2010).

32. Drury, A. J. *et al.* Deciphering the State of the Late Miocene to Early Pliocene Equatorial Pacific. *Paleoceanogr. Paleoclimatology* **33**, 246–263, DOI: 10.1002/2017PA003245 (2018).

33. Sangiorgi, F. *et al.* Southern Ocean warming and Wilkes Land ice sheet retreat during the mid-Miocene. *Nat. Commun.* **9**, 317, DOI: 10.1038/s41467-017-02609-7 (2018).

34. Levy, R. *et al.* Antarctic ice sheet sensitivity to atmospheric CO2 variations in the early to mid-Miocene. *Proc. Natl. Acad. Sci.* **113**, 3453–3458, DOI: 10.1073/pnas.1516030113 (2016).